Gerami *et al. International Journal of Advanced Structural Engineering* 2013, **5**:9
http://www.advancedstructeng.com/content/5/1/9

International Journal of Advanced Structural Engineering
a SpringerOpen Journal

ORIGINAL RESEARCH **Open Access**

Nonlinear seismic vulnerability evaluation of irregular steel buildings with cumulative damage indices

Mohsen Gerami, Yahya Sharbati* and Abbas Sivandi-Pour

Abstract

Measuring structural damage during earthquakes has always been a challenging problem for earthquake engineers. Various damage indices are proposed with the objective of quantifying the structural damage in prototype and model structures subjected to seismic excitation. In this study, seismic vulnerability of irregular steel buildings is assessed in three dimensions considering effects of the panel zone, which has not been considered in recent studies of the field of seismic vulnerability. The buildings are modeled with different storeys and irregular plans. Seismic performance of buildings was assessed in life-safety and collapse-prevention levels. Cumulative functions of damage indices are applied in the nonlinear dynamic analysis of buildings in the near-field ground motions. It is concluded that participation rates of deformation and energy in the damage of irregular buildings are 74.5% and 25.5%, respectively. Severe damage and collapse due to seismic dissipated energy occurred in the initial storeys of low-rise buildings and in the middle storeys of high-rise buildings.

Keywords: Seismic vulnerability, Damage index, Performance level, Irregular buildings, Panel zone

Introduction

Damage and detraction in recent earthquakes have shown that even though buildings designed according to recent codes and regulations have performed well from the viewpoint of the safety of human lives, the level of damage to the buildings and the consequent economic losses are unexpectedly high. In order to assess the reliability of structures subjected to ground motions, it is necessary to evaluate failure modes, which lead to cyclic deterioration in strength, stiffness, and energy dissipation. Many researchers have tried to determine numerical functions in order to express the partial and total vulnerability of structures. These functions are considered as the first step of the seismic rehabilitation of the structure. More recent damage functions showed the more realistic view to structural damage. One of the main topics of debate in vulnerability evaluation of structures is selecting the most appropriate damage functions for a special structure to show a structural situation more realistically (Foutch and Yun 2002; Kalkan and Kunnath 2007; Gerami and Sivandi-Pour 2008; Nethercot 2011). In a study, Elnashai (2006) evaluated seismic vulnerability of structures. He introduced different methods and tools for evaluating vulnerability of buildings. Shibin et al. (2010) assessed vulnerability and control of structures based on the performance levels. They suggested a probable approach for seismic evaluation of buildings. (Bojórquez et al. 2010) introduced an energy damage index for multi-degree-of-freedom steel buildings. Their model was developed by complementing the results obtained by experimental and analytical investigation on steel frame elements regarding the distribution of plastic demands on several steel frames. Pitocco (2011) studied the information technology in the context of evaluation of steel building vulnerability. He suggested some methods for modification of damaged buildings. Determination of most damage indices involves complicated and time-consuming computations that are neither economical nor feasible in concurrent structural engineering practice. Cumulative damage indices are usually modeled either by using a low-cycle fatigue formulation, in which damage is taken as a function of the accumulated plastic deformation, or by inserting a term related to the dissipated hysteretic

* Correspondence: ya.sharbati@gmail.com
Faculty of Civil Engineering, Semnan University, Semnan 3513119111, Iran

energy in the damage model (Kunnath and Chai 2004; Poljanšek and Fajfar 2008; Karimi et al. 2011). No study was found on seismic vulnerability of buildings considering panel zone and irregularity. In this study, the panel zone is considered and irregular buildings are modeled three dimensionally. Cumulative damage indices considering deformation and dissipated energy (ductility, energy, Park-Ang) were used. To evaluate the seismic vulnerability of models, near-field records of Tabas, Northridge, and Kobe earthquakes were used.

Method

Design of buildings

Models in this study include steel buildings with three bays in five types of 4, 7, 10, 15, and 20 storeys. The height of each storey was 3.5 m, and the length of each bay is 4.5 m. The buildings were designed based on the Iranian code of practice for seismic-resistant design of buildings (Standard 2800) and LRFD method of AISC (2005) (see Appendix). The loads and load combinations were determined according to ASCE/SEI 7–05 (2005). The buildings have irregular plans as shown in Figure 1.

A lateral resistant system is a moment frame in the *X*-direction and a dual system of moment frame and bracing in the *Y*-direction. IPE sections for beams, IPB sections for columns, and UNP sections for braces were used in the modeling and design.

Nonlinear modeling of elements

For nonlinear dynamic analysis, using OpenSees, an open-source finite element platform has been developed at the University of California-Berkeley for earthquake performance assessment (Mazzoni et al. 2006). Fy, *E*, *G*, and strain hardness were considered to be 2,400 kg/cm^2, 2.1×10^6, 807,692.30, and 3%, respectively. For nonlinear dynamic analysis, a nonlinear beam column element is used, which is based on the non-iterative (or iterative) force formulation, and considers the distribution of plasticity along the element. In order to do nonlinear dynamic analysis, each element was divided into ten parts. In these parts, the stresses and strains were derived from three points at the top, middle, and bottom corners of the section by which cyclic energy dissipation in each frame element was calculated.

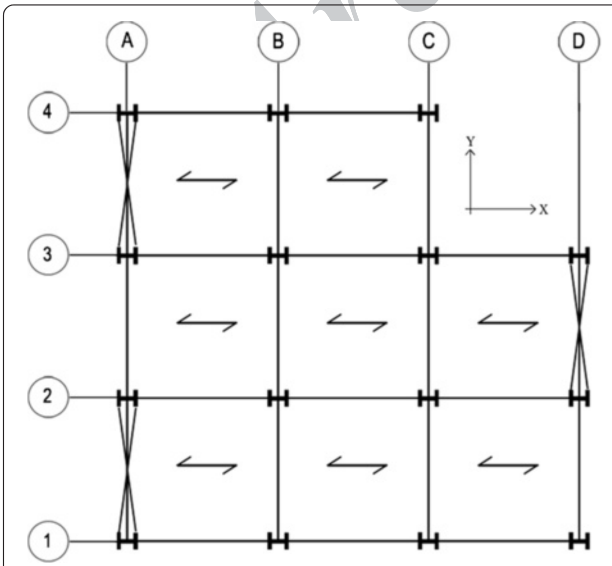

Figure 1 Plan of buildings.

Modeling of connections and panel zone

During seismic events, connections in steel buildings would experience a large amount of stress and deformation demands due to their critical position in the structure. Panel zone is the web area of beam-to-column connection delineated by the extension of beam and column flanges through the connection, transmitting moment through a shear panel. Panel zones are assigned to joints to model the flexibility of beam-column connections. Correct modeling of the beam-column connections is very important in the nonlinear analysis of moment frames. Four models were used in the steel buildings in order to model the connections of beam to column:

1. *Linear model*. This model is suitable for designing a moment-resisting frame. Although the model shows reasonable results for design, it cannot accurately forecast the distribution of the inelastic frame element forces.
2. *Elastic model with modeling panel zone*. The beam and column will be connected to the panel zone by a rigid link. Stiffness of the panel zone is modeled as a spring.
3. *Nonlinear model*. Yielding of frame elements is higher than that of the elastic model. This method is currently used in the modeling of buildings. Modeled springs will remain rigid until the section reaches plastic moment.
4. *Nonlinear model with modeling panel zone*. Three approaches can be used in the modeling of the panel zone. The first is to join with a nonlinear spring. In the second one, two springs are used: one for rigidity of the panel zone and the other for average strength of beam and the panel zone. In the third approach, the panel zone is modeled with eight rigid elements (Krawinkler 2000; Lignos 2008; Kim and Engelhardt 2002; Asgarian et al. 2010).

In this study, a nonlinear model with modeling of the panel zone was used in modeling the joints in OpenSees. Two nonlinear springs were modeled. Beams and columns are jointed by the rigid link in the panel zone.

Although the rigid link increases joint stiffness, the modeled spring in the panel zone causes flexibility. A rotational spring with trilinear behavior is then utilized to tie the beam and column together. The rigid links stiffen the structure, but the panel zone spring adds flexibility. The net result would lead to a relatively stiffer assembly than that of the center-line model. Since it is stiffer, it would help in satisfying the drift design criteria. This model has been shown in Figure 2.

The accurate description of the panel zone stiffness is very important in the analyses leading to the estimation of the fundamental period and of the expected frame drift. Spring stiffness of the panel zone is obtained from the following relation:

$$K_\theta = \frac{M_y}{\theta_y} \tag{1}$$

$$M_y = V_y.d_b = 0.55F_y d_c t d_b \tag{2}$$

$$\theta_y = \gamma_y = \frac{F_y}{\sqrt{3}G} \tag{3}$$

where F_y represents the yield strength of panel zone, G represents the shear module, d_c represents the column height, d_b is beam height, and t is thickness of panel zone.

Near-field ground motion records

Near-field problems have become an important topic for both seismologists and earthquake engineers. The characteristics of near-field records of an earthquake are quite different from the usual far-field records. After the original recognition of their differences in the Port Hueneme earthquake in 1957, a lot of inhabited structures and lifeline systems were damaged in the major earthquakes which happened in the following year. The special characteristics of near-field ground motions are directly related to the earthquake source mechanism, rupture direction relative to the site, and slip direction of the rupture fault (Gioncu 1998; Tirca et al. 2003; Alavi and Krawinkler 2004; Brun et al. 2004; Bray and Rodriguez-Marek 2004; Li and Xie 2007; Gerami et al. 2012; Monavari and Massumi 2012). In the present research work, three near-field earthquake records (Tabas, Kobe, and Northridge) were chosen. Models were loaded under longitudinal and transversal components of each record. Records were analyzed, and the difference between damages and function of different damage indices in each storey of the buildings were evaluated and compared. The specifications of records are presented in Table 1 and Figure 3.

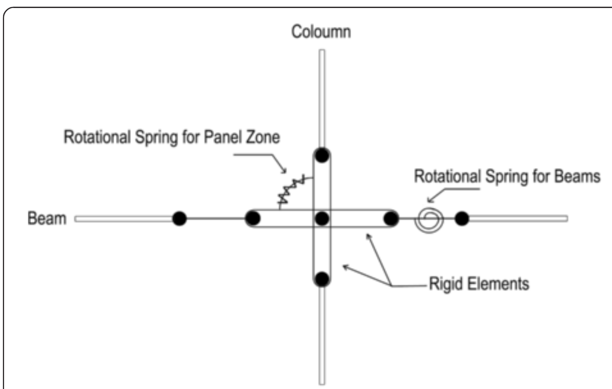

Figure 2 Modeling of panel zone in OpenSees.

Seismic performance assessment

Two hazard levels of 1 and 2 were defined for seismic performance evaluation and structural vulnerability. The hazard level 1 (Basic Safety Earthquake (BSE)-1) is determined based on 10% probability of the event during 50 years that is equivalent to a return period of 475 years. The hazard level 2 (BSE-2) is determined based on 2% probability of the event during 50 years that is equivalent to a return period of 2475 years.

Relative displacement of the storeys is one of the general standards used in studying the performance of structures. The maximum relative displacement of a building's roof in each different level for different earthquakes has been presented in Table 2.

If the frame elements are controlled by deformation, this index can be calculated. The beams are assumed to be displacement-controlled frame elements. As with the columns, if the ratio of P/P_{cl} is less than 0.5, the control is measured by displacement. In the parameters required in the determination of ductility, yield and maximum rotation of frame elements were considered. Maximum rotation of frame elements in life safety (LS) and collapse prevention (CP) performance levels is given in Table 3.

The determination of target displacement of models using coefficient method according to FEMA 356 (2000) is shown in Table 4. This method estimates the target displacement, providing a direct numerical process for calculating the displacement demands.

Buildings were loaded with live and dead loads for gravity loading, and then laterally loaded. For each building, the total weight of the building, total height, fundamental translational mode period, roof displacement,

Table 1 Specification of ground motions

Earthquake	Location	Date	PGA (g)		Ms
			Long	Trans	
Tabas	Iran	1978	0.85	0.83	7.8
Kobe	Japan	1995	0.75	0.36	6.9
Northridge	USA	1979	0.82	0.6	6.5

PGA, peak ground acceleration; Long, longitudinal; Trans, transversal.

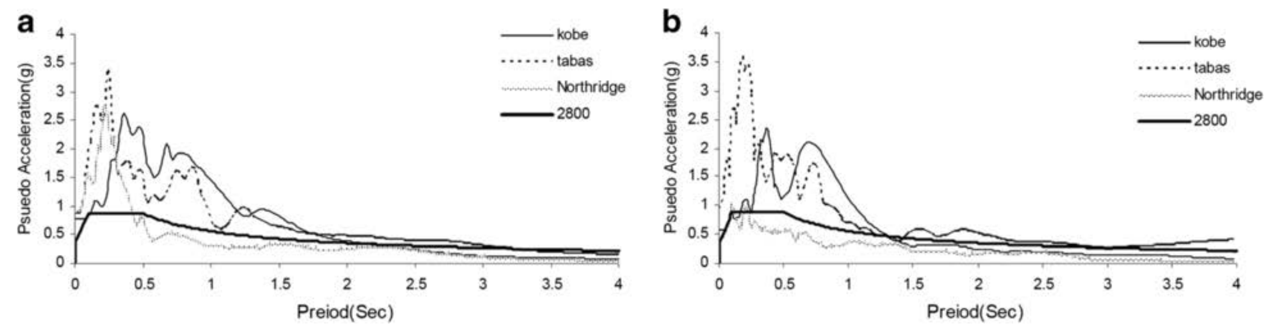

Figure 3 Spectral accelerations of ground motion records. (**a**) Longitudinal component and (**b**) transversal component.

and base shear were recorded. Figure 4 illustrates the capacity curve of models in the *X*-direction under uniform and dynamic load pattern.

In Figure 4, *W* represents the weight, *H* represents the height, and Δroof represents the maximum displacement of models. Maximum displacement of models in BSE-1 and BSE-2 are shown in Figure 5.

Results

Damage index is known to be a standard measure in evaluating structural damage. Damage indices are usually normalized so that their value is equal to zero when there is no damage and is equal to unity when total collapse or failure occurs. Damage indices can involve a combination of one or more variables in its determination. Damage indices are applicable to different types of structural systems under different loadings and are defined based on parameters indicating economic conditions.

Ductility damage index

The simplest definition for a damage function belongs to ductility damage index. Energy dissipation by elements is not considered in ductility damage index, and only maximum deformation is used while expressing the damage amount. This parameter shows the ratio of maximum deformation and yield deformation of frame elements. Equation 4 shows the ductility damage index.

$$\mathrm{DI}_{\mathrm{Ductility}} = \frac{\theta_m}{\theta_y} \tag{4}$$

In this relation, θ_{m} represents the maximum rotation of frame elements during earthquake and θ_{y} denotes the yield rotation of elements. Figure 6 shows a schematic curve for calculating the ductility factor.

A ductility factor of less than 1 indicates elastic response, and the values of more than 1 show non-elastic responses, if there is monotonic loading. This damage index is presented in Figures 7, 8, and 9.

Maximum value of the ductility damage index in frame elements is presented in Table 5. The mean value of ductility damage indices in beams in BSE-1 and BSE-2 are 4.3 and 6.4, respectively. This value is 8.3 for columns and 11.9 for BSE-1 and BSE-2. From the average values, it can be conclude that the deformation of the columns is 93% higher than the BSE-1 beams and 87% higher than BSE-2.

Energy damage index

The amount of energy dissipation in each frame element is considered as an index in the evaluation of performance and structural damage. This function is defined based on

Table 2 Maximum relative displacement in two hazard levels

Models	Maximum displacement (cm)					
	BSE-1			BSE-2		
	Tabas	Northridge	Kobe	Tabas	Northridge	Kobe
4	19.8	20	20.5	21.5	29.5	22.7
7	17.48	29.72	26.14	27.78	38.2	35.05
10	44.6	36.91	51.05	73.32	49.91	80.16
15	59.51	44.9	62.68	88.82	45.33	78.56
20	63.35	44.51	56.69	117.94	58.19	64.46

Table 3 Maximum rotation of frame elements in performance levels

Models	Maximum rotation of columns (rad)				Maximum rotation of beams (rad)
	Uniform distribution		Spectral distribution		
	LS	CP	LS	CP	
4	0.008	0.014	0.005	0.008	0.0097
7	0.005	0.007	0.008	0.005	0.0097
10	0.0063	0.0090	0.0219	0.0106	0.011
15	0.0028	0.0034	0.0036	0.0046	0.0079
20	0.0031	0.0038	0.0049	0.0064	0.0079

Table 4 Target displacement of models in performance levels

Models	Target displacement in *X*-direction (cm)				Target displacement in *Y*-direction (cm)			
	Uniform load pattern		Dynamic load pattern		Uniform load pattern		Dynamic load pattern	
	LS	CP	LS	CP	LS	CP	LS	CP
4	17.87	32.92	20.10	32.92	5.80	9.49	5.80	9.49
7	33.03	54.04	39.91	65.30	13.33	21.82	13.33	21.82
10	37.88	61.98	40.58	66.41	22.16	36.26	22.16	36.26
15	48.05	78.63	58.07	95.02	44.02	72.04	44.02	72.04
20	57.51	94.11	69.49	113.71	59.18	96.85	59.18	96.85

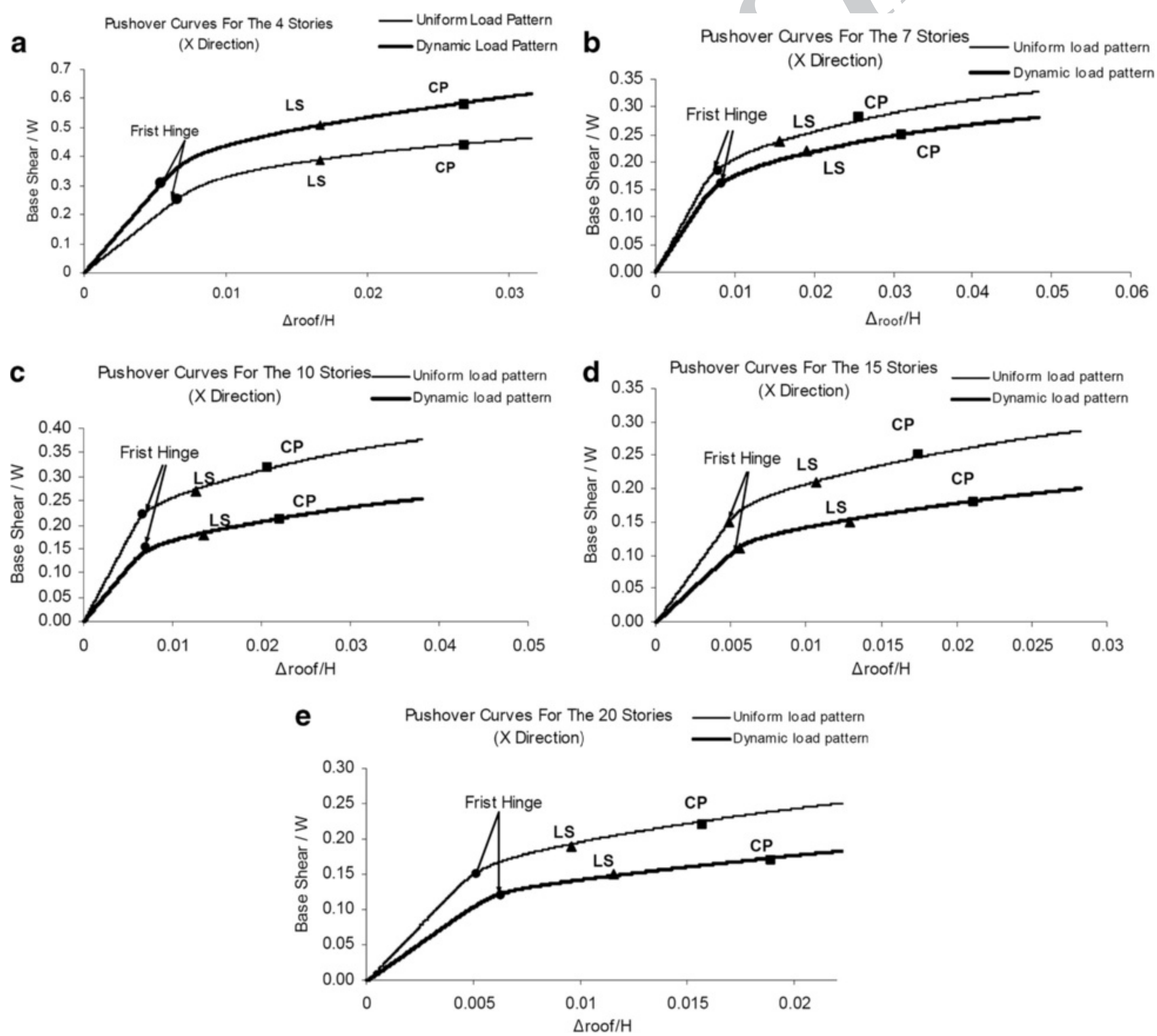

Figure 4 Pushover curve of models. (**a**) 4, (**b**) 7, (**c**) 10, (**d**) 15, and (**e**) 20 storeys.

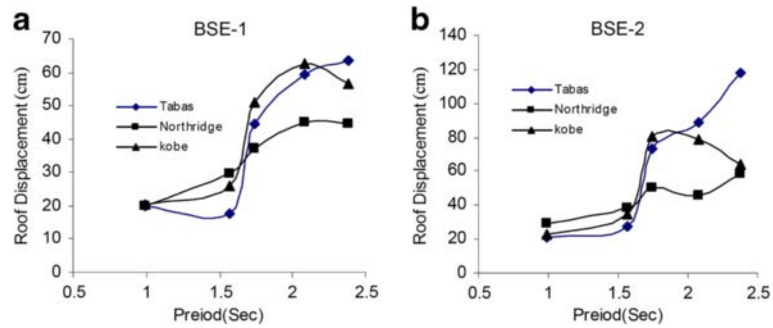

Figure 5 Maximum roof displacement variations in (a) BSE-1 and (b) BSE-2.

hysteretic energy dissipated by elements. Energy damage index considers only the energy absorbed by elements and does not include their deformations. Regarding energy dissipated in damage index function, the effects of earthquake duration and damage aggregation are included. Energy damage index is expressed according to the following relation:

$$\mathrm{DI}_{\mathrm{Energy}} = \frac{\mathrm{EH}/F_y\Delta_y}{\left(\Delta_u/\Delta_y - 1\right)} \tag{5}$$

where EH is the energy dissipated by the system, and Δ_y is yield limit strength of the frame element. Energy damage indices of the models have been compared for different earthquakes in Figures 10, 11, and 12.

Results of this index showed that most damages in low-rise buildings occurred in initial storeys and in high-rise buildings occurred in intermediate storeys. The maximum value of energy damage index in frame elements is given in Table 6.

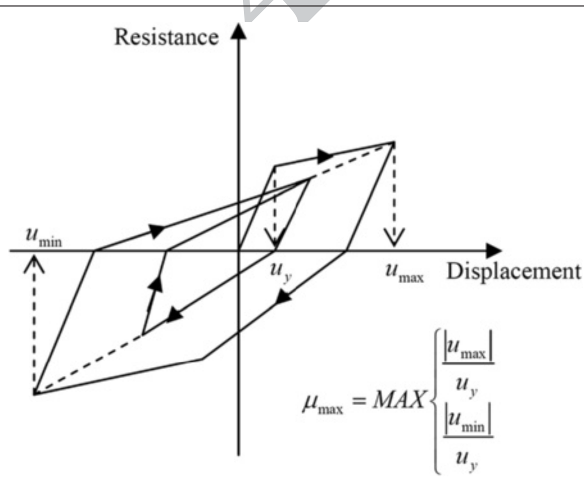

Figure 6 Maximum ductility factor.

The mean value of energy damage indices in beams in BSE-1 and BSE-2 are 0.87 and 1.43, respectively. For the columns, these values increase to 1.2 and 1.83 for BSE-1 and BSE-2. It can be observed that energy dissipated by columns in earthquakes is 38% higher in BSE-1 and 28% higher in BSE-2 compared to the beams.

Park-Ang damage index

The Park-Ang damage index considers the effects of both parameters of maximum deformation and dissipated energy in damage evaluation (Park et al. 1984).

The relation of this index can be expressed as follows:

$$\mathrm{DI}_{\mathrm{Park-Ange}} = \frac{\Delta_m}{\Delta_u} + \beta\frac{\mathrm{EH}}{F_y\Delta_u} \tag{6}$$

where Δ_m is the maximum deformation of the element, Δ_u is the ultimate deformation, and β is a model constant parameter.

In this research, the value of β is 0.15, indicating the amount of energy dissipated in the damage range. This damage index is one of the functions that offer a certain range for describing the physical concept of the damage level. A comparison of this damage index for different earthquakes is shown in Figures 13, 14, and 15.

Maximum value of the Park-Ang damage index in frame elements is presented in Table 7.

The average of the Park-Ang damage index in beams for BSE-1 and BSE-2 is 0.75 and 1.26, respectively. This value is 0.55 and 1.1 for columns.

Discussion

Maximum values of damage indices are shown in Figures 16, 17, and 18.

There was no remarkable difference in response of buildings under records for 4- and 7-storey buildings. Increase in storeys caused noticeable changes in the results of records, so this difference will reach a peak in

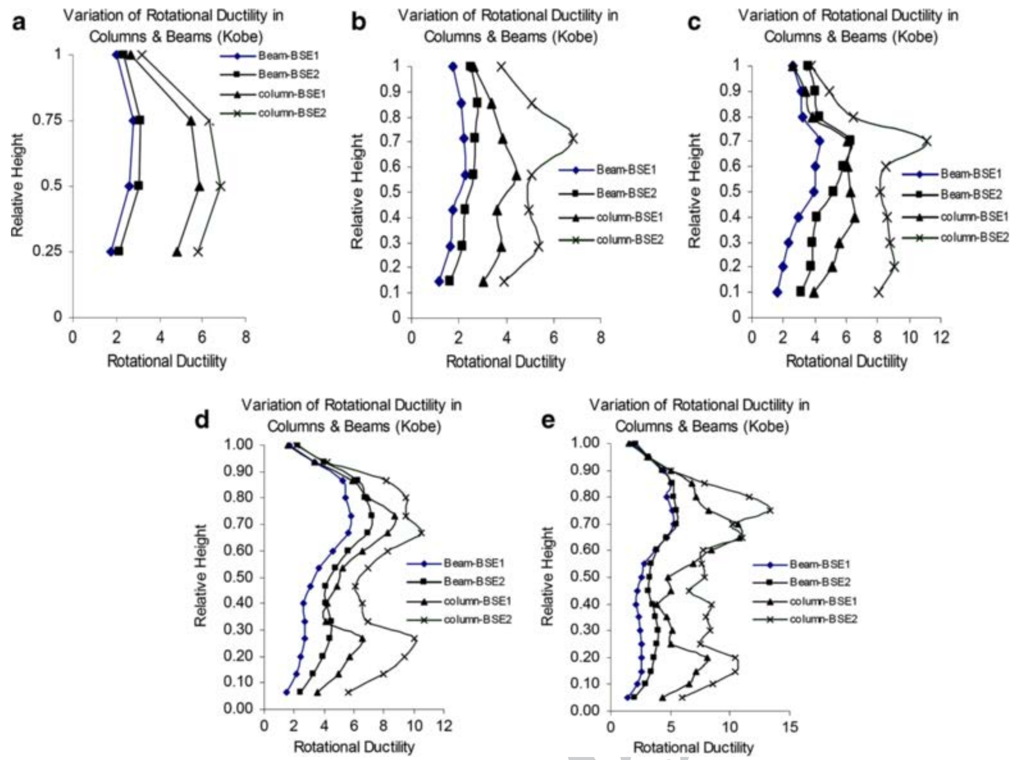

Figure 7 Ductility damage index in Kobe earthquake. For models (**a**) 4, (**b**) 7, (**c**) 10, (**d**) 15, and (**e**) 20 storeys.

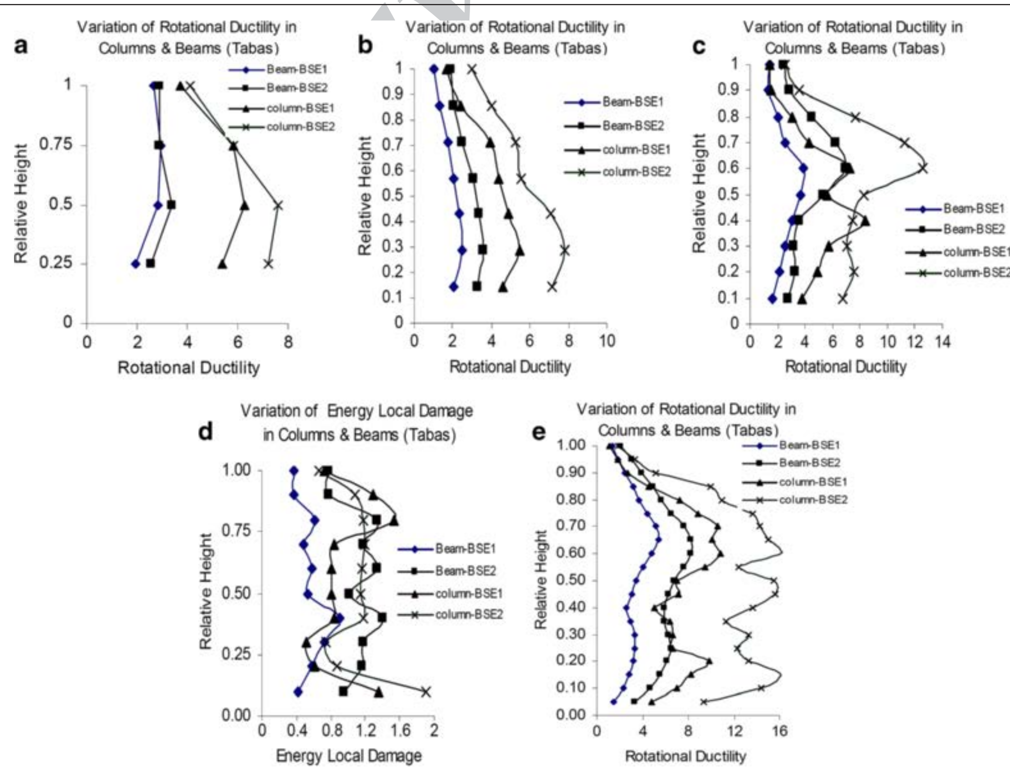

Figure 8 Ductility damage index in Tabas earthquake. For models (**a**) 4, (**b**) 7, (**c**) 10, (**d**) 15, and (**e**) 20 storeys.

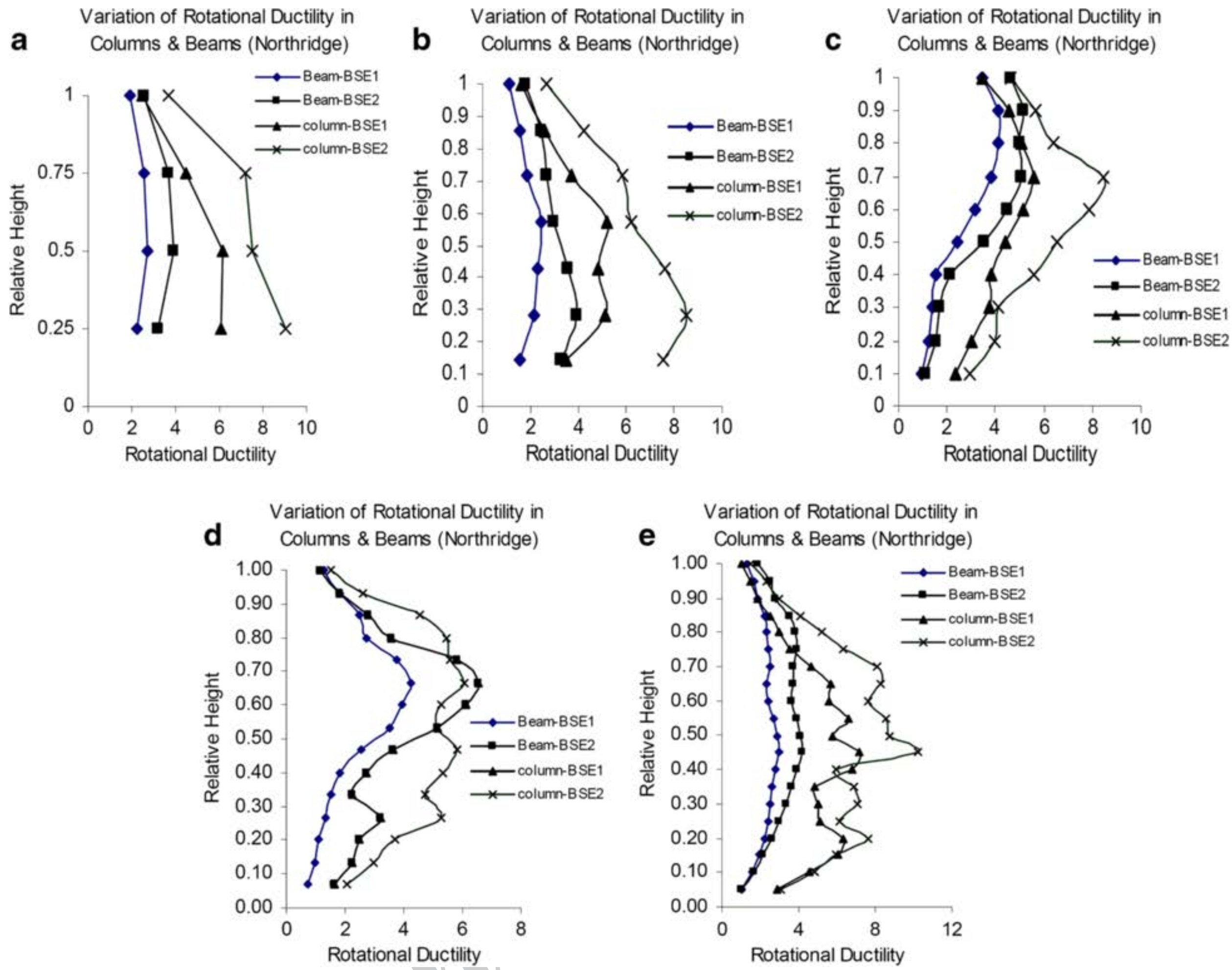

Figure 9 Ductility damage index in Northridge earthquake. For models (**a**) 4, (**b**) 7, (**c**) 10, (**d**) 15, and (**e**) 20 storeys.

the 15-storey model. The maximum value of ductility damage index belonged to the 15-storey model in hazard level 1, and its value was 1.23 for Tabas earthquake. In hazard level 2, the highest value of this index was equal to 1.74, similar to the first hazard level.

Table 5 Maximum value of ductility damage index in frame elements

Models	Beams		Columns	
	BSE-1	BSE-2	BSE-1	BSE-2
4	2.92	3.91	6.3	9.02
7	2.51	3.89	6.12	8.55
10	4.32	6.98	8.39	12.55
15	6.43	8.97	9.48	13.39
20	5.39	8.29	10.88	16.08
Average	4.30	6.40	8.30	11.90

As with the energy damage index, the highest energy absorption belonged to the 20-storey model under Tabas earthquake in hazard level 1. The minimum value of energy absorption was that of the 7-storey model. In hazard level 2, the highest energy absorption in Tabas earthquake was for the 15-storey model.

Participation rates of deformation and energy are compared in Figure 19.

Figure 19 illustrates the deformation as the most effective factor in the damage of buildings. Participation rates of deformation in damage of low-rise and high-rise buildings are 73% and 76%, respectively. Energy has 27% and 24% participation rates in damage.

Conclusions

In order to assess the reliability of structures subjected to ground motions, it is necessary to evaluate failure modes leading to cyclic deterioration. This paper has investigated the vulnerability of irregular buildings in

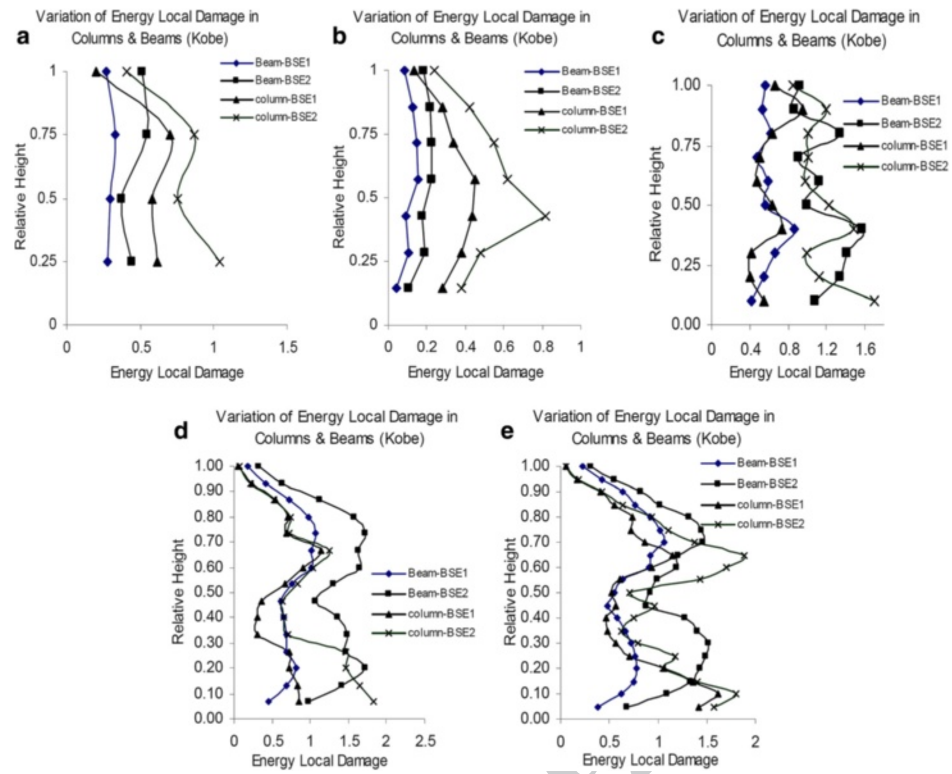

Figure 10 Energy damage index in Kobe earthquake. For models (**a**) 4, (**b**) 7, (**c**) 10, (**d**) 15, and (**e**) 20 storeys.

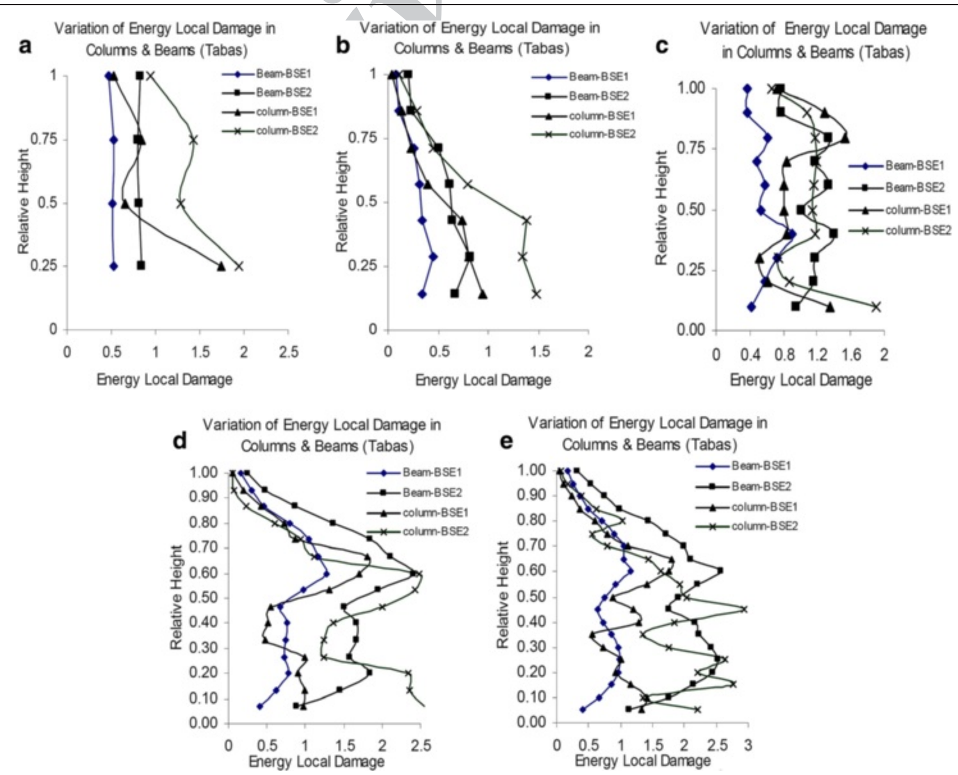

Figure 11 Energy damage index in Tabas earthquake. For models (**a**) 4, (**b**) 7, (**c**) 10, (**d**) 15, and (**e**) 20 storeys.

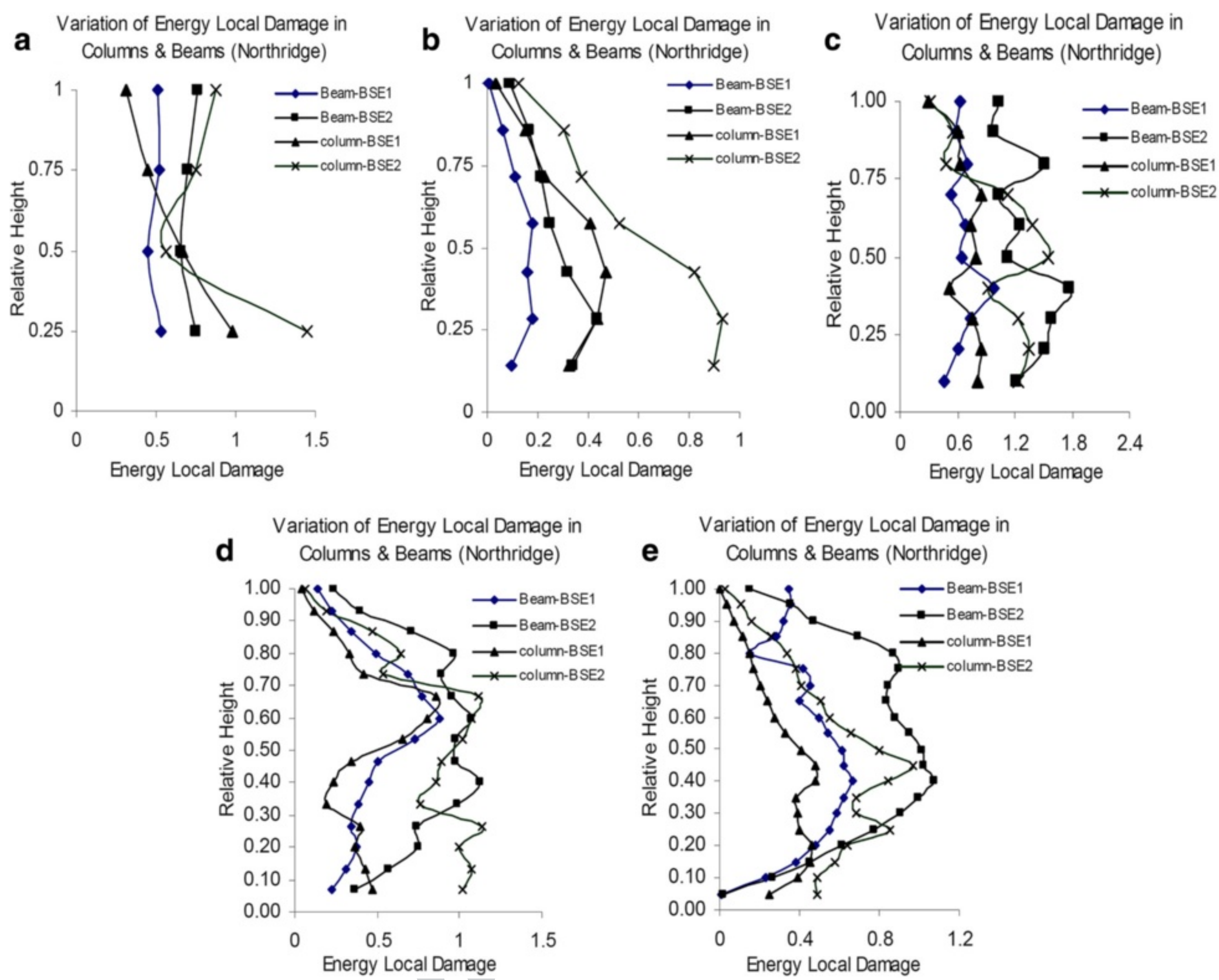

Figure 12 Energy damage index in Northridge earthquake. For models (**a**) 4, (**b**) 7, (**c**) 10, (**d**) 15, and (**e**) 20 storeys.

near-field earthquakes using cumulative damage indices (ductility, energy, Park-Ang). In this study, the panel zone is considered, and irregular buildings are modeled three dimensionally. In order to do nonlinear dynamic analysis, each element was divided into ten parts. In these parts, the stresses and strains were derived from three points at the top, middle, and bottom corners of the section.

Table 6 Maximum value of energy damage index in frame elements

Models	Beams		Columns	
	BSE-1	BSE-2	BSE-1	BSE-2
4	0.53	0.84	0.7	0.86
7	0.45	0.35	0.82	0.94
10	0.97	0.99	1.53	1.89
15	1.28	2.41	1.81	2.55
20	1.15	2.56	1.18	2.93

By increasing storeys in buildings, the value of required ductility in top storeys increased. Vulnerability of columns in the first storey in all buildings exceeded the allowable value. Deformation of columns was 93% in BSE-1 and 87% in BSE-2 which is higher than the beams in earthquakes.

In the most vulnerable storeys of low-rise and high-rise buildings, the values of dissipated energy are 34% and 26%, respectively. Severe damage and collapse occurred in the initial storeys of low-rise buildings and middle storeys of high-rise buildings due to seismic dissipated energy. For BSE-1 and BSE-2, energy dissipated in columns during earthquakes is 38% and 28% more than beams, respectively.

The maximum and minimum value of the Park-Ang damage index occurred in high-rise and low-rise

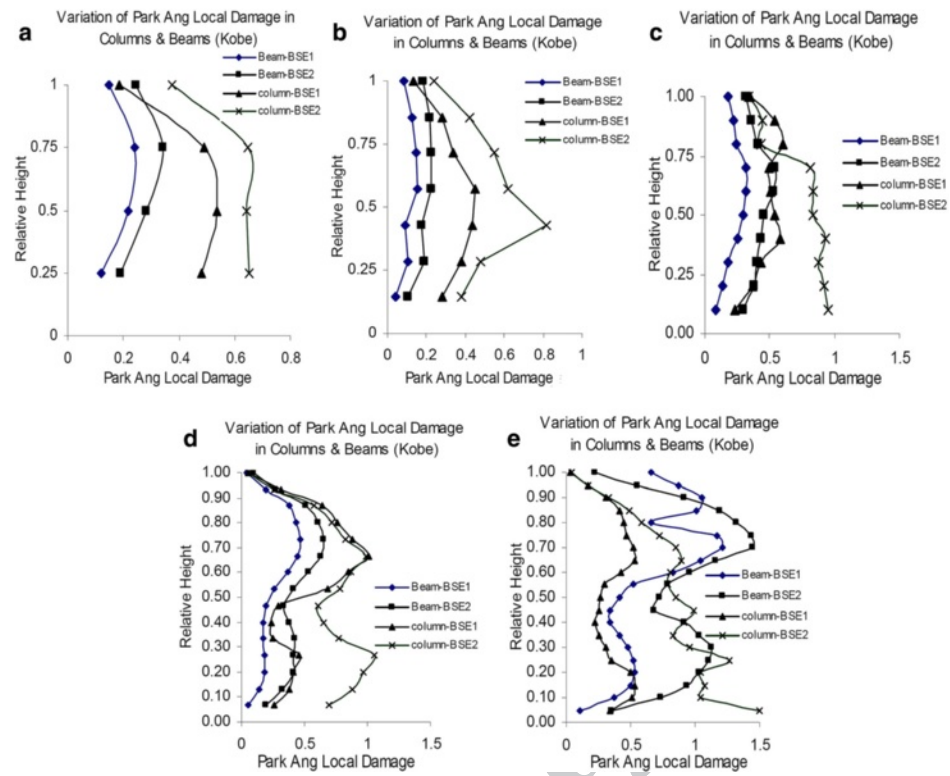

Figure 13 Park-Ang damage index in Kobe earthquake. For models (**a**) 4, (**b**) 7, (**c**) 10, (**d**) 15, and (**e**) 20 storeys.

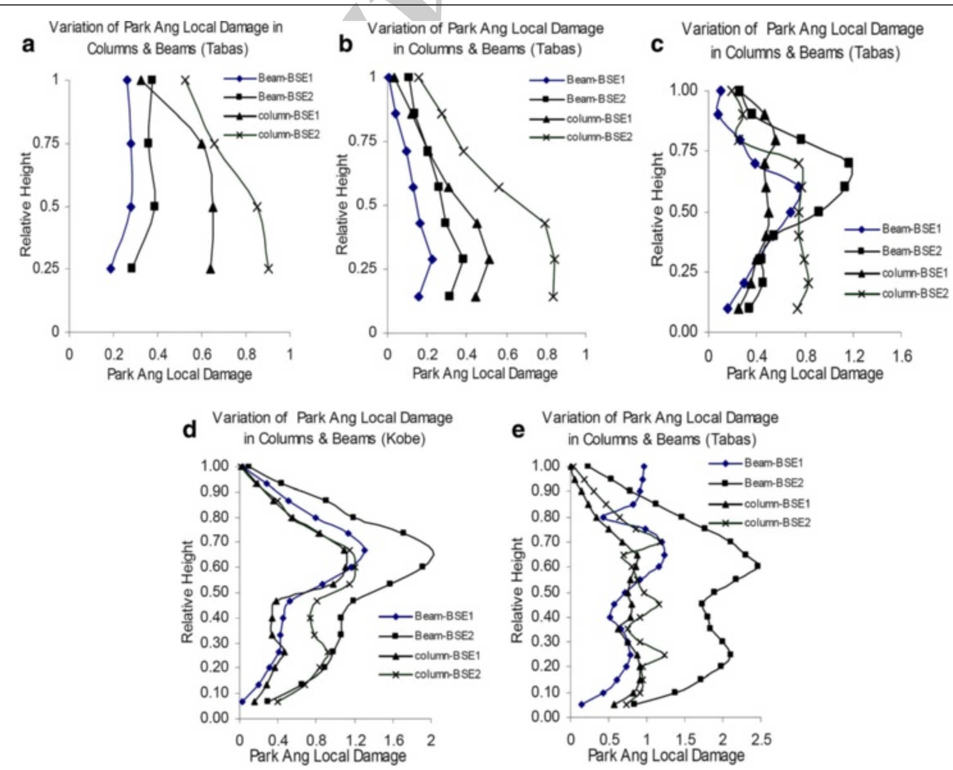

Figure 14 Park-Ang damage index in Tabas earthquake. For models (**a**) 4, (**b**) 7, (**c**) 10, (**d**) 15, and (**e**) 20 storeys.

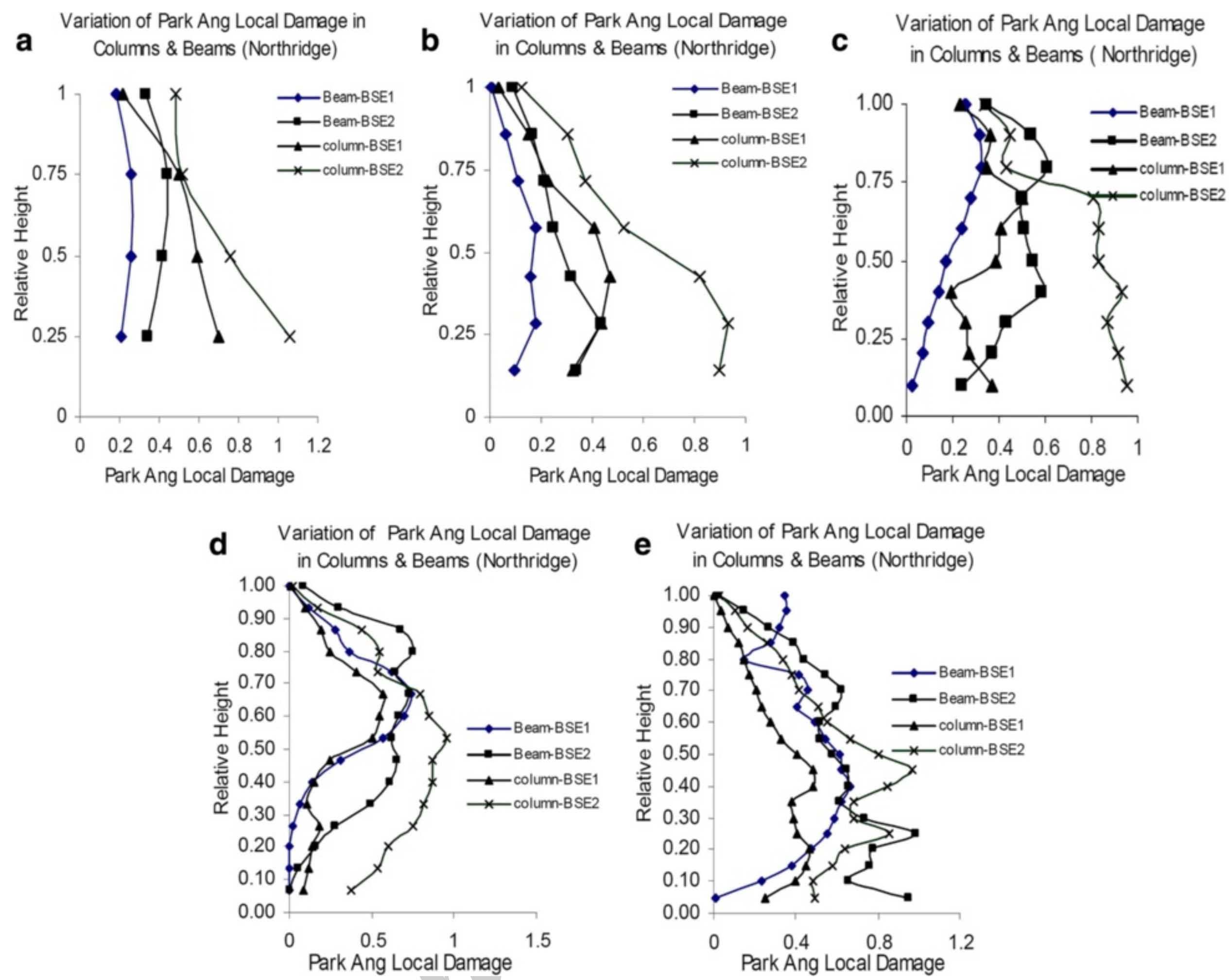

Figure 15 Park-Ang damage index in Northridge earthquake. For models (**a**) 4, (**b**) 7, (**c**) 10, (**d**) 15, and (**e**) 20 storeys.

buildings, respectively. The mean value of the Park-Ang damage index for beams in BSE-1 and BSE-2 was 0.75 and 1.26, respectively. This value was 0.55 and 1.1 for columns.

Participation rates of deformation and energy in damage of irregular low-rise buildings were 73% and 27%, respectively. Deformation and energy had 76% and 24% participation rates in damage of irregular high-rise buildings, respectively.

Table 7 Maximum value of Park-Ang damage index in frame elements

Models	Beams		Columns	
	BSE-1	BSE-2	BSE-1	BSE-2
4	0.28	0.43	0.65	0.9
7	0.22	0.43	0.47	0.95
10	0.75	1.18	0.61	0.96
15	1.3	1.79	0.11	1.21
20	1.24	2.47	0.91	1.49

Appendix

Iranian seismic code

Every decade or so, a major earthquake strikes Iran. The 2003 Bam earthquake was the last major earthquake in Iran. Traditional buildings in Iran, especially in the rural areas, have very little resistance to earthquakes of higher magnitude. After numerous major earthquakes, in particular that of 1963 in Bouein Zahra and 1978 in Tabas, the Iranian government began the upgrading of the code of practice for earthquake protection. The Iranian Building and Housing Research Centre further revised the code, construction and design, and the updated and revised Iranian code for seismic-resistant design.

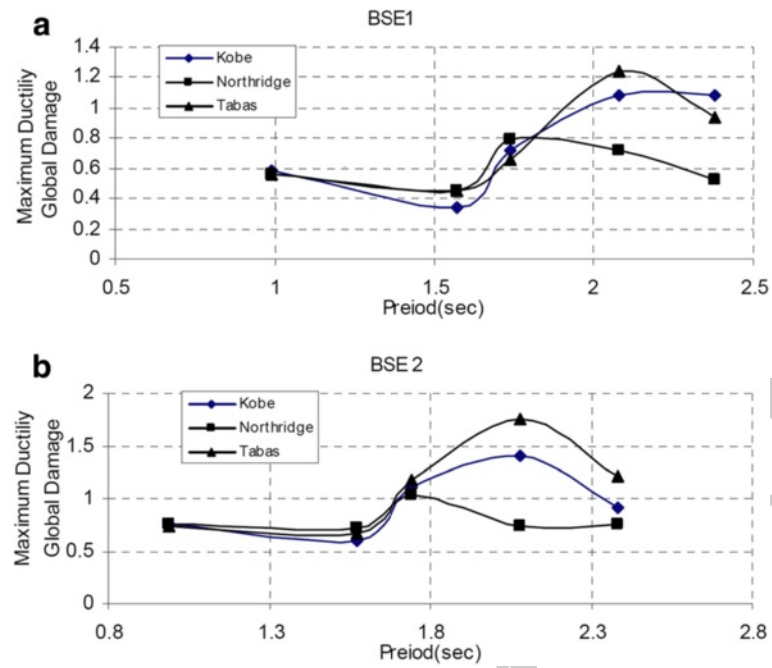

Figure 16 Maximum ductility damage index variations of storeys in (a) BSE-1 (b) BSE-2.

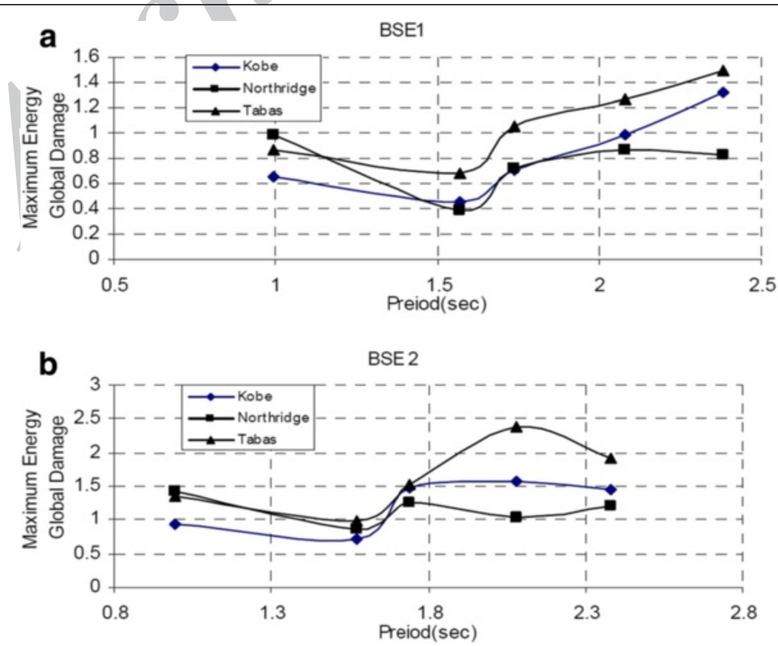

Figure 17 Maximum energy damage index variations of storeys in (a) BSE-1 (b) BSE-2.

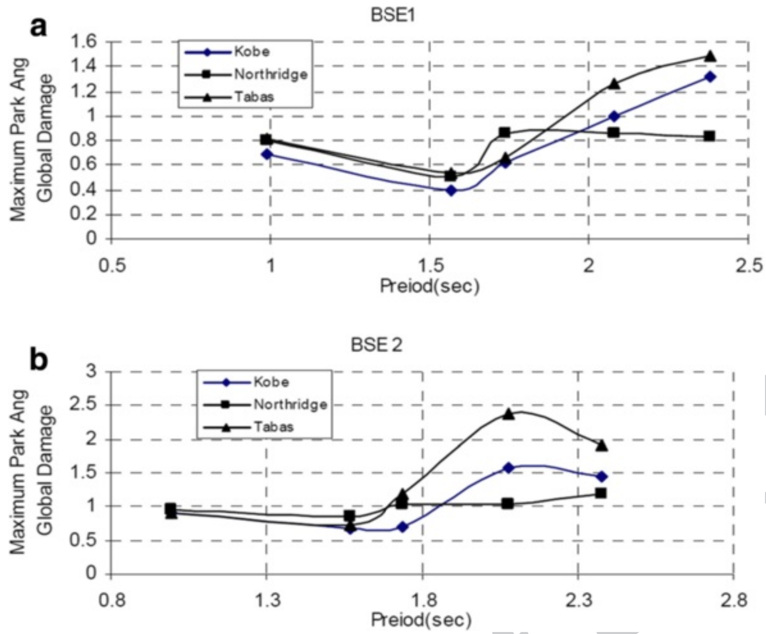

Figure 18 Maximum Park-Ang damage index variations of storeys in (a) BSE-1 (b) BSE-2.

The design details of buildings according to the Iranian Seismic Code 2800 and the different seismic regions are categorized based on relevant seismic hazard analyses. As per Iranian Seismic Code 2800, earthquake lateral forces can be calculated using the following methods depending on the structure:

- Equivalent static analysis method
- Dynamic analysis method

An equivalent static analysis method is allowed just for regular structures which are not taller than 50 m or not irregular ones which are taller than 18 m. Other types of buildings must be designed using the dynamic analysis method. Since in this study the structures are irregular and are taller than 18 m, a dynamic analysis method is used in the design of buildings (Building and Housing Research Center 1999,2005; Asgarian et al. 2010; Gioncu and Mazzolani 2011).

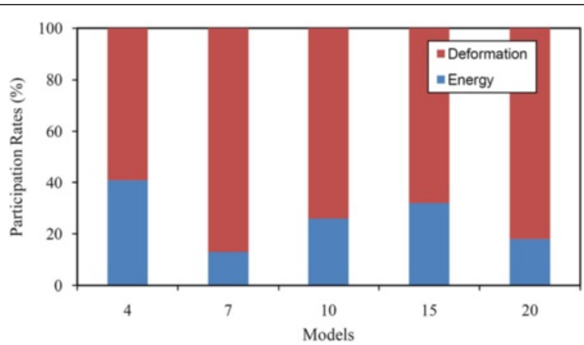

Figure 19 Participation rates of deformation and energy in damage.

Competing interests
The authors declare that they have no competing interests.

Authors' contributions
MS defined the main theme and objective of the study and explained the research methodology. YS carried out the modeling and analysis, obtained the numerical results which are presented in the research work, and prepared the first draft of the paper. AS controlled the obtained numerical results, edited and finalized the manuscript, and participated in the global revision and discussion of the review performed. All authors read and approved the final manuscript.

Authors' information
MG is an assistant professor at the Faculty of Civil Engineering in Semnan University. YS is an MSc in Earthquake Engineering from Semnan University. AS is a PhD candidate in Earthquake Engineering at Semnan University.

Received: 20 August 2012 Accepted: 24 February 2013
Published: 4 April 2013

References
AISC (2005) Seismic provisions for structural steel buildings. Standard ANSI/AISC. American Institute of Steel Construction, Chicago
Alavi B, Krawinkler H (2004) Behavior of moment-resisting frame structures subjected to near-fault ground motions. J Earthquake Eng Struct Dynam 33(6):65–86
ASCE/SEI 7–05 (2005) Minimum design loads for buildings and other structures. American Society of Civil Engineers, Reston
Asgarian B, Sadrinezhad A, Alanjari P (2010) Seismic performance evaluation of steel moment resisting frames through incremental dynamic analysis. J Constr Steel Res 66(2):178–90
Bray JD, Rodriguez-Marek A (2004) Characterization of forward-directivity ground motions in the near-fault region. Int J Soil Dynam Earthquake Eng 24(11):815–828

Brun M, Reynouard JM, Jezequel L, Ile N (2004) Damaging potential of low-magnitude near field earthquakes on low-rise shear walls. Int J Soil Dynam Earthquake Eng 24(8):587–603
Bojórquez E, Reyes-Salazar A, Terán-Gilmore A, Ruiz SE (2010) Energy-based damage index for steel structures. J Steel Compos Struct 10(4):343–360
Elnashai AS (2006) Assessment of seismic vulnerability of structures. J Constr Steel Res 62(11):1134–1147
FEMA 356 (2000) "Prestandard and Commentary for the Seismic Rehabilitation of Buildings", prepared by the American Society of Civil Engineers for the Federal Emergency Management Agency. FEMA, Washington, DC
Foutch DA, Yun SY (2002) Modeling of steel moment frames for seismic loads. J Constr Steel Res 58(5):529–564
Gerami M, Sivandi-Pour A (2008) "Introduction of earthquake loads amplification factor in design of seismic resistant steel buildings and comparison in various regulations". In: 1st national conference on retrofitting, Yazd, Iran (in Persian). 26–28 August 2008
Gerami M, Sivandi-Pour A, Pourmeydani E (2012) "Assessment of effect of earthquake vertical component on seismic performance of ductile steel seismic resistant systems". In: 9th international congress on civil engineering, Isfahan, Iran (in Persian). 8–10 May 2012
Gioncu V (1998) Ductility criteria for steel structures. J Constr Steel Res 46(1–3):443–444
Gioncu V, Mazzolani FM (2011) Earthquake engineering for structural design. Spon Press, London and New York
Building and Housing Research Center (1999) Iranian code of practice for seismic resistant design of buildings, vol 2800, 2nd edition. Building and Housing Research Center, Tehran
Building and Housing Research Center (2005) Iranian code of practice for seismic resistant design of buildings, vol 2800, 3rd edition. Building and Housing Research Center, Tehran
Kalkan E, Kunnath SH (2007) Assessment of current nonlinear static procedures for seismic evaluation of buildings. J Eng Struct 29(3):305–316
Karimi M, Hosseinzadeh N, Hosseini F, Kazem N, Kazem H (2011) Seismic vulnerability evaluation of pipe rack supporting structures in a petrochemical complex. Int J Adv Struct Eng 3(1):111–120
Kim KD, Engelhardt MD (2002) Monotonic and cyclic loading models for panel zones in steel moment frames. J Constr Steel Res 58(5–8):605–35
Krawinkler H (2000) The state-of-the-art report on system performance of moment resisting steel frames subjected to earthquake ground shaking, FEMA 355c. Federal Emergency Management Agency, Washington, DC
Kunnath SK, Chai YH (2004) Cumulative damage-based inelastic cyclic demand spectrum. J Earthquake Eng Struct Dynamics 33(4):499–520
Li S, Xie L (2007) Progress and trend on near field problems in civil engineering. Acta Seismologica Sinica 20(1):105–114
Lignos D (2008) Sidesway collapse of deteriorating structural systems under seismic excitations. Ph.D. thesis. Stanford University
Mazzoni S, McKenna F, Scott MH, Fenves GL (2006) The Open System for Earthquake Engineering Simulation (OpenSEES) user command-language manual. Pacific Earthquake Eng. Research Center, University of Califorinia, Berkeley. http://opensees.berkeley.edu
Monavari B, Massumi A (2012) Estimating displacement demand in reinforced concrete frames using some failure criteria. Int J Adv Struct Eng 4(4). doi:10.1186/2008-6695-4-4
Nethercot DA (2011) Design of building structures to improve their resistance to progressive collapse. J procedia Eng 14:1–13
Park YJ, Ang AH-S, Wen YK (1984) "Seismic damage analysis and damage-limiting design of RC buildings". Structural Research Series No.516. University of Illinois, Urbana
Pitocco M (2011) Information technology and management of diagnostics for analysis of seismic vulnerability in buildings. J Procedia Comput Sci 3:352–360
Poljanšek K, Fajfar P (2008) "A new damage model for the seismic damage assessment of reinforced concrete structures". In: 14th world conference on earthquake engineering, Beijing, China. 12–17 October 2008
Shibin L, Lili X, Maosheng G, Ming L (2010) Performance-based methodology for assessing seismic vulnerability and capacity of buildings. J Earthq Eng Vib 9 (2):157–165
Tirca L-D, Foti D, Diaferio M (2003) Response of middle-rise steel frames with and without passive dampers to near field ground motions. J Eng Struct 25(2):169–179

doi:10.1186/2008-6695-5-9
Cite this article as: Gerami *et al.*: Nonlinear seismic vulnerability evaluation of irregular steel buildings with cumulative damage indices. *International Journal of Advanced Structural Engineering* 2013 **5**:9.